iScience

CellPress
OPEN ACCESS

Article

Hepatokine ITIH3 protects against hepatic steatosis by downregulating mitochondrial bioenergetics and *de novo* lipogenesis

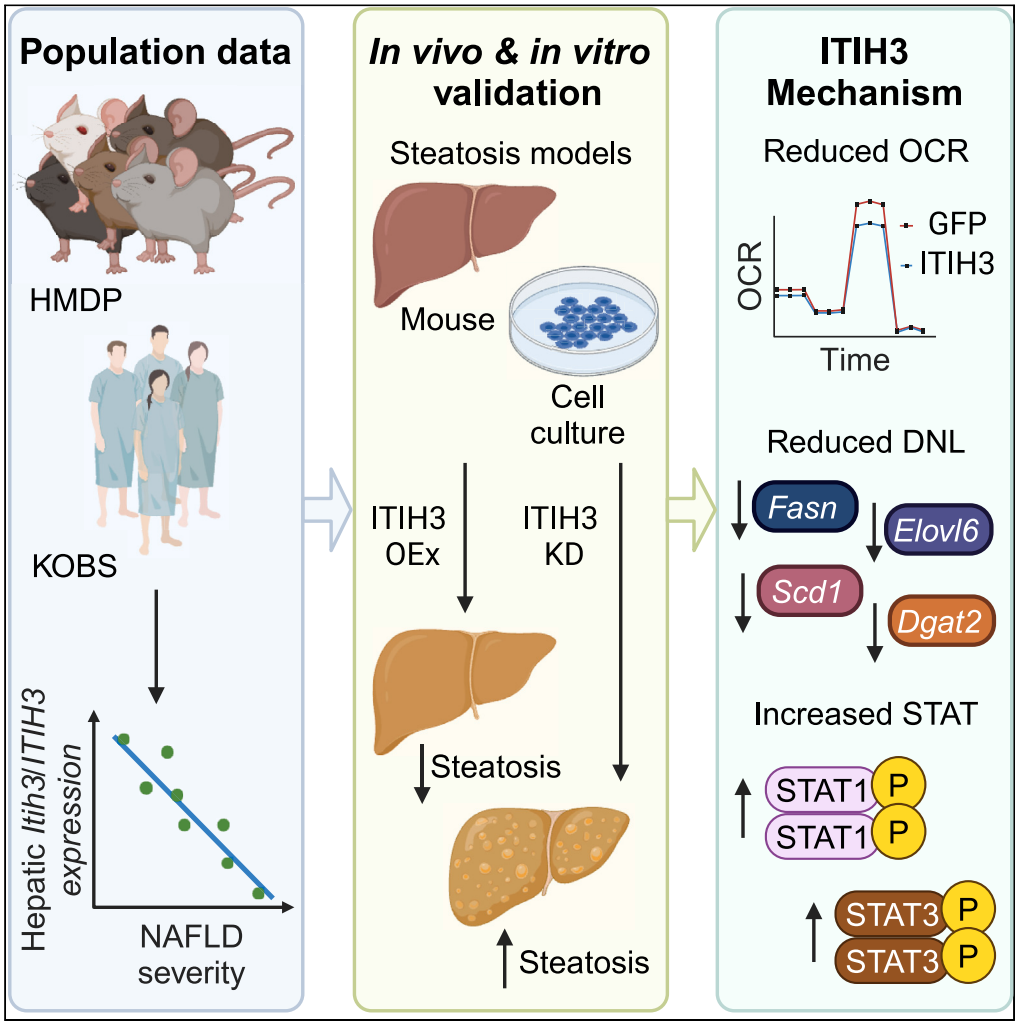

Noble Kumar Talari, Ushodaya Mattam, Dorota Kaminska, ..., Päivi Pajukanta, Jussi Pihlajamäki, Karthickeyan Chella Krishnan

chellakn@ucmail.uc.edu

Highlights

In both mice and humans, hepatokine ITIH3 is inversely related to NAFLD severity

ITIH3 overexpression rescues both mice and hepatocytes from steatosis

ITIH3 reduced mitochondrial respiration and downregulated *de novo* lipogenesis

ITIH3 increased STAT1 signaling and *Stat3* expression

Talari et al., iScience 27, 109709
May 17, 2024
https://doi.org/10.1016/j.isci.2024.109709

iScience

CellPress
OPEN ACCESS

Article

Hepatokine ITIH3 protects against hepatic steatosis by downregulating mitochondrial bioenergetics and *de novo* lipogenesis

Noble Kumar Talari,[1,9] Ushodaya Mattam,[1,9] Dorota Kaminska,[2,3] Irene Sotomayor-Rodriguez,[4] Afra P. Rahman,[4] Miklós Péterfy,[5] Päivi Pajukanta,[6,7] Jussi Pihlajamäki,[3,8] and Karthickeyan Chella Krishnan[1,10,*]

SUMMARY

Recent studies demonstrate that liver secretory proteins, also known as hepatokines, regulate normal development, obesity, and simple steatosis to non-alcoholic steatohepatitis (NASH) progression. Using a panel of ~100 diverse inbred strains of mice and a cohort of bariatric surgery patients, we found that one such hepatokine, inter-trypsin inhibitor heavy chain 3 (ITIH3), was progressively lower in severe non-alcoholic fatty liver disease (NAFLD) disease states highlighting an inverse relationship between *Itih3/ITIH3* expression and NAFLD severity. Follow-up animal and cell culture models demonstrated that hepatic ITIH3 overexpression lowered liver triglyceride and lipid droplet accumulation, respectively. Conversely, ITIH3 knockdown in mice increased the liver triglyceride in two independent NAFLD models. Mechanistically, ITIH3 reduced mitochondrial respiration and this, in turn, reduced liver triglycerides, via downregulated *de novo* lipogenesis. This was accompanied by increased STAT1 signaling and *Stat3* expression, both of which are known to protect against NAFLD/NASH. Our findings indicate hepatokine ITIH3 as a potential biomarker and/or treatment for NAFLD.

INTRODUCTION

The most common cause of chronic liver disease on a global scale is non-alcoholic fatty liver disease (NAFLD).[1–6] NAFLD is an umbrella term ranging from simple steatosis (fat accumulation in hepatocytes) to complex non-alcoholic steatohepatitis (NASH), fibrosis and cirrhosis, eventually leading to hepatocellular carcinoma (HCC).[1–3] An important feature of NAFLD is their differential prevalence and disease phenotypes between males and females.[2,7–12] Given that obesity and insulin resistance are strongly associated with NAFLD,[2,6,13,14] the prevalence of NAFLD is rising concurrently with the obesity epidemic, creating a significant current and future healthcare challenge. Despite this, factors governing the progression of the disease or prospective drug targets are yet unknown. To this end, we used an integrative multiomics approach using a well-characterized mouse population, the hybrid mouse diversity panel (HMDP),[15] and identified a liver secreted protein, ITIH3 as a potential candidate protein involved in NAFLD pathogenesis.

Secretory proteins, cytokines and hormones have paracrine or endocrine functions on neighboring cells or other tissues, maintaining systemic nutrient and energy homeostasis. Hence, the abundance and structure of these chemical messengers change in response to the normal/disease conditions. Several proteins circulating in the blood are synthesized by the liver and are altered during the different stages of liver pathologies. Recent works demonstrated that genes encoding secretory proteins are abundantly expressed in livers of people with type 2 diabetes.[16] Furthermore, genes encoding fibrinogenic factors, angiogenic factors, and redox-associated factors are reported to regulate the pathophysiology of type 2 diabetes.[17,18] Therefore, the metabolic disturbance in the liver often regulates the whole-body energy metabolism. Indeed, several liver-derived secretory proteins or hepatokines affect the metabolism of peripheral organs.[19–21]

Inter-α-trypsin inhibitors (ITI) are plasma protease inhibitors that are assembled from light and heavy chain precursor proteins. ITI genes are transcribed in the liver as light chain and heavy chain polypeptides.[22] A single light chain with a combination of different heavy chains, such as ITIH1, ITIH2, ITIH3, ITIH4, and ITIH5, forms a mixture of complex proteins. So far, the difference in their rearrangements results in different

[1]Department of Pharmacology and Systems Physiology, University of Cincinnati College of Medicine, Cincinnati, OH, USA
[2]Department of Medicine, Division of Cardiology, University of California Los Angeles, Los Angeles, CA, USA
[3]Institute of Public Health and Clinical Nutrition, Department of Clinical Nutrition, University of Eastern Finland, Kuopio, Finland
[4]Medical Sciences Baccalaureate Program, University of Cincinnati College of Medicine, Cincinnati, OH, USA
[5]Department of Basic Medical Sciences, Western University of Health Sciences, Pomona, CA, USA
[6]Department of Human Genetics, David Geffen School of Medicine at UCLA, University of California Los Angeles, Los Angeles, CA, USA
[7]Institute for Precision Health, David Geffen School of Medicine at UCLA, University of California Los Angeles, Los Angeles, CA, USA
[8]Department of Medicine, Endocrinology and Clinical Nutrition, Kuopio University Hospital, Kuopio, Finland
[9]These authors contributed equally
[10]Lead contact
*Correspondence: chellakn@ucmail.uc.edu
https://doi.org/10.1016/j.isci.2024.109709

functional polypeptides namely, urinary trypsin inhibitor (UTI), inter-α-trypsin inhibitors (ITI), pre-α-inhibitor (PαI), or inter-α-trypsin inhibitor family heavy chain related protein (IHRP).[23] ITI proteins act as hyaluronic acid binding proteins,[24] anti-inflammatory agents,[25] extracellular matrix stabilizers[23] and inhibitors of tumor cell invasion.[26] These liver secreted protease inhibitors play important roles during normal development, tissue remodeling,[27,28] cancer,[29] insulin resistance,[30] and HCC.[31] Previous studies have demonstrated the importance of hepatokines in hepatic steatosis, but there is not much progress made toward the identification and/or functional importance of ITI proteins in hepatic steatosis or NAFLD. In addition, comparative analysis of mouse liver and plasma proteome revealed a strong correlation between both in pathology.[32] Taken together, it is imperative to further our understanding on hepatokines in the context of liver pathology to diagnose, treat and prevent hepatic diseases.

Our current focus is to investigate the role of hepatokine ITIH3 on NAFLD pathogenesis. To this end, we used both mouse and human populations and show that ITIH3 is strongly and negatively associated with the disease progression suggesting a protective role against NAFLD/NASH development. Using both loss- and gain-of-function strategies in mouse and cell culture experiments, we further confirmed that ITIH3 negatively regulates liver lipid accumulation. Furthermore, we identified ITIH3 to protect against NAFLD by regulating both mitochondrial metabolism and *de novo* lipogenesis (DNL).

RESULTS

ITIH3 is a potential candidate gene for protection against NAFLD

We had earlier used an integrative multiomics approach using transcriptomic data from approximately 100 different mouse strains called HMDP and identified several "key driver" genes underlying hepatic TG accumulation.[15] Using similar approaches, here we show that ITIH3 is a potential "key driver" gene, that is strongly correlated with other inflammatory and coagulation factors (Figure 1A). Particularly, we found STAT3, a transcription factor widely known to ameliorate steatosis and liver fibrosis[33–35] and LRG1, a secreted hepatokine that was reported to inhibit M1 polarization of hepatic macrophages to alleviate NASH,[36] to be positively correlated; whereas CXCL10, a pro-inflammatory cytokine reported to increase steatosis and NASH[37] and KRT23, a reported biomarker for NASH and progression to HCC,[38] to be negatively correlated with hepatic *Itih3* expression. Additionally, we found another ITI family gene namely, ITIH4, to be positively correlated with hepatic *Itih3* expression. Follow-up investigations on livers isolated from HMDP strains maintained on chow (healthy), high fat-high sucrose HF/HS (steatosis)[39] and western (NASH/fibrosis)[40] diets revealed that as NAFLD progresses, liver *Itih3* expression significantly decreases (Figure 1B). Focusing on the HMDP strains maintained on HF/HS diet revealed us that liver *Itih3* expression was negatively correlated with liver triglyceride (TG) levels (Figure 1C). Furthermore, immunoblot analyses of C57BL/6J mice revealed that ITIH3 protein levels in the liver decreased with diet-induced NAFLD/NASH progression (Figure S1). Taken together, we reasoned that loss in hepatic *Itih3* expression worsens the NAFLD conditions.

To further explore the gene networks and pathways associated with hepatic *Itih3* expression, we computed *Itih3* correlated hepatic genes (listed in Table S1) from HMDP strains maintained on HF/HS diet (bicor > |±0.3|; p < 1E-05). Follow up enrichment analysis by DAVID[41] and ToppGene[42] results in identification of NAFLD-related metabolic pathways such as cholesterol metabolism, mitochondria, fatty acid metabolism and TCA cycle (Figure 1D); and NAFLD-related disease terms such as fatty liver, liver cirrhosis, steatohepatitis, dyslipidemia, and NAFLD (Figure 1E). Finally, to understand the clinical relevance of hepatic *ITIH3* expression in human NAFLD/NASH, we used the RNA-seq data from a total of 262 liver biopsies from the Kuopio Obesity Surgery (KOBS) cohort. We found a negative correlation between hepatic *ITIH3* expression and NAFLD/NASH-related phenotypes such as steatosis grade (Figure 1F), fibrosis stage (Figure 1G; Figure S2) and triglyceride levels (Figure 1H). Taken together, since our population studies in both mice and human revealed that hepatic *Itih3/ITIH3* expression was negatively correlated with NAFLD/NASH phenotypes and associated with mitochondria and metabolism gene networks, we hypothesized that hepatic ITIH3 protects against NAFLD and were further interested to investigate the ITIH3's role in NAFLD.

ITIH3 attenuates hepatic steatosis both *in vivo* and *in vitro*

To functionally validate the protective role of ITIH3 against liver steatosis, we performed fructose water or HF/HS diet induced steatosis models in 8-week-old male C57BL/6J mice using both silencing and/or overexpression strategies via AAV8 vectors. For ITIH3 knockdown studies, liver specific AAV vectors harboring shRNA against *ffLuc* (control) or *Itih3* was used; for overexpression studies, liver specific AAV vectors harboring cDNAs of GFP (control) or ITIH3 was used. The validity of these strategies is shown in Figure S3. All these animals were subjected to either 15% fructose water for 12 weeks or HF/HS diet for 8 weeks. We noted that both ITIH3 knockdown and overexpression did not alter the body weights in both steatosis models (Figures 2A, 2C, and 2E). We next analyzed the hepatic lipid profiles in the presence or absence of ITIH3. We noticed that knocking down ITIH3 significantly increased the intrahepatic triglyceride content in both steatosis models (Figures 2B and 2D) without altering total cholesterol (TC), unesterified cholesterol (UC), and phospholipids (PL). To further confirm this, we observed a significant reduction in the liver TG content with no changes in TC, UC, and PL in ITIH3 overexpression mice (Figure 2F). Furthermore, H&E staining demonstrated that ITIH3 overexpression significantly lowered liver lipid droplet accumulation (Figure S4). However, we did not observe any significant differences with liver weights, plasma TG or TC levels (Figure S5). We also found no significant differences in fasting plasma glucose, insulin, or homeostatic model assessment for insulin resistance (HOMA-IR) (Figure S6).

We next explored ITIH3's role in *in vitro* cell culture models by overexpressing *Itih3* plasmid in oleic acid treated AML12 liver cells. Oil red O staining was performed to analyze the lipid content. We report that ITIH3 overexpression results in reduction of total lipid droplet content in comparison with GFP overexpression as measured by Oil red O staining (Figures 2G and 2H). We did not perform any *in vitro* knockdown studies as AML12 cells inherently had very low ITIH3 expression. Taken together, we conclude that ITIH3 confers hepatoprotection against steatosis both *in vivo* and *in vitro*.

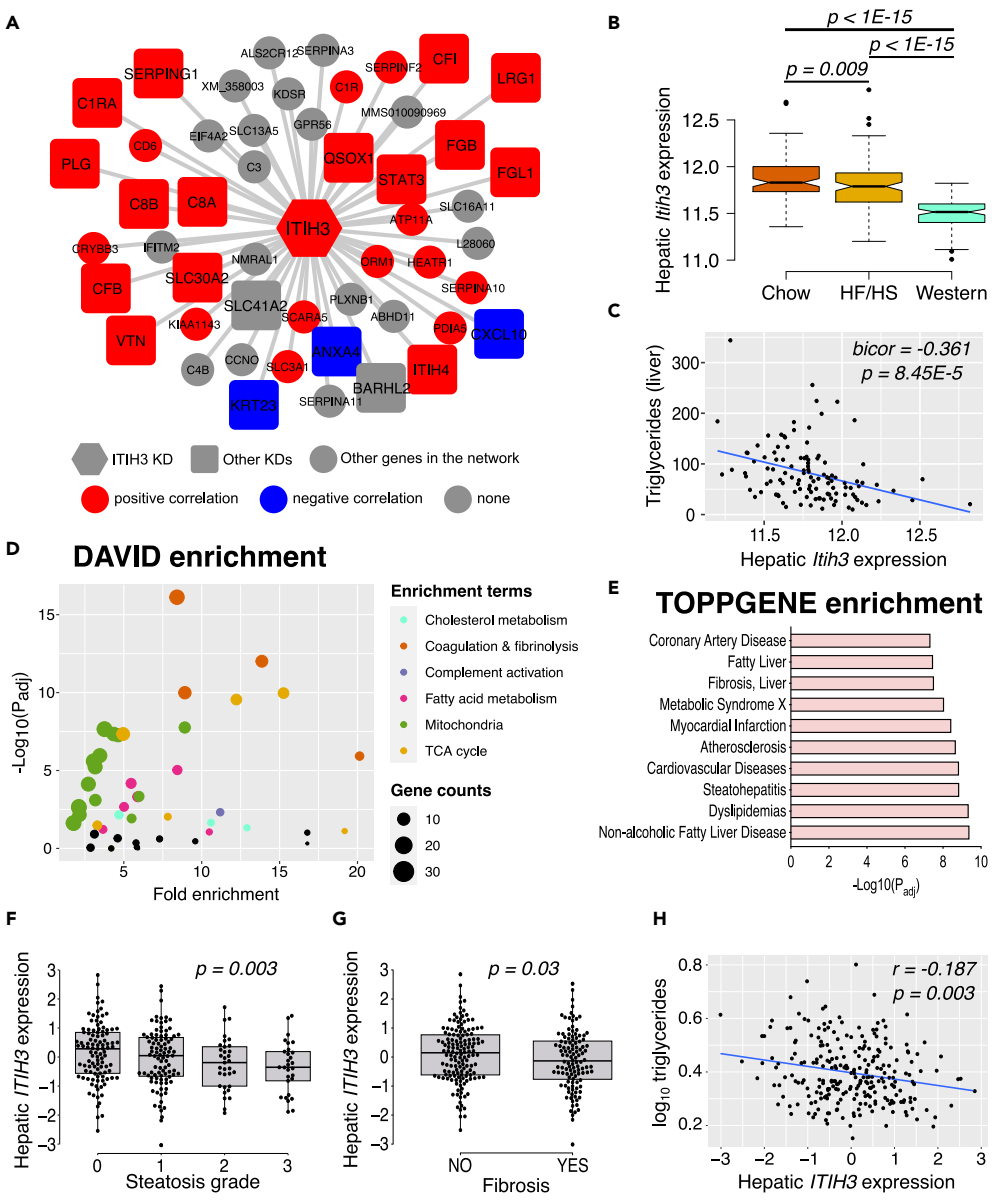

Figure 1. ITIH3 is negatively associated with NAFLD/NASH in both mice and humans

(A) Overlay of HMDP bicorrelation directionality on ITIH3 key driver (KD) network from our previous study.[15] ITIH3 is represented in hexagon shape, other key driver genes are represented in square shapes, and the rest of the network genes are represented in circle shapes. Red represents positive and blue represents negative correlation with liver *Itih3* expression from HMDP strains maintained on HF/HS diet (n = 113 HMDP strains).

(B) Liver *Itih3* expression from HMDP strains maintained on chow (n = 96 HMDP strains) or HF/HS (n = 113 HMDP strains) or western (n = 102 HMDP strains) diet.

(C) Correlation plot between hepatic *Itih3* expression and triglyceride in HMDP strains maintained on HF/HS diet (n = 113 HMDP strains).

(D) DAVID pathway and (E) ToppGene disease enrichment analyses of highly correlated HMDP liver genes (listed in Table S1) with liver *Itih3* expression (bicor > |±0.3|; p < 1E-05). Hepatic *ITIH3* expression from KOBS cohort (n = 262) grouped by (F) steatosis grade and (G) Fibrosis.

(H) Correlation plot between hepatic *ITIH3* expression and triglycerides. Data are presented as median and interquartile range (boxplots). p values were calculated by (A and C) bicor; (B) one-factor ANOVA corrected by post-hoc "Holm-Sidak's" multiple comparisons test; (F and G) ANCOVA corrected for age, BMI, and sex; (H) partial correlation adjusting for age, BMI, and sex. HMDP, hybrid mouse diversity panel; bicor, biweight midcorrelation; BMI, body mass index.

ITIH3 protects against steatosis by lowering mitochondrial respiration

Several studies have demonstrated that mitochondrial respiration is elevated during hepatic steatosis due to high substrate availability and ATP demand resulting in hyperactive OXPHOS phenotypes.[15,43] Chronic hyperactive OXPHOS phenotypes are maladaptive leading to oxidative damages. Therefore, lowering mitochondrial respiration is the key to rescue from steatosis as we have demonstrated earlier.[15,44] Given that our DAVID gene enrichment analyses revealed hepatic *Itih3* expression to be associated with mitochondria and TCA cycle (Figure 1D), we

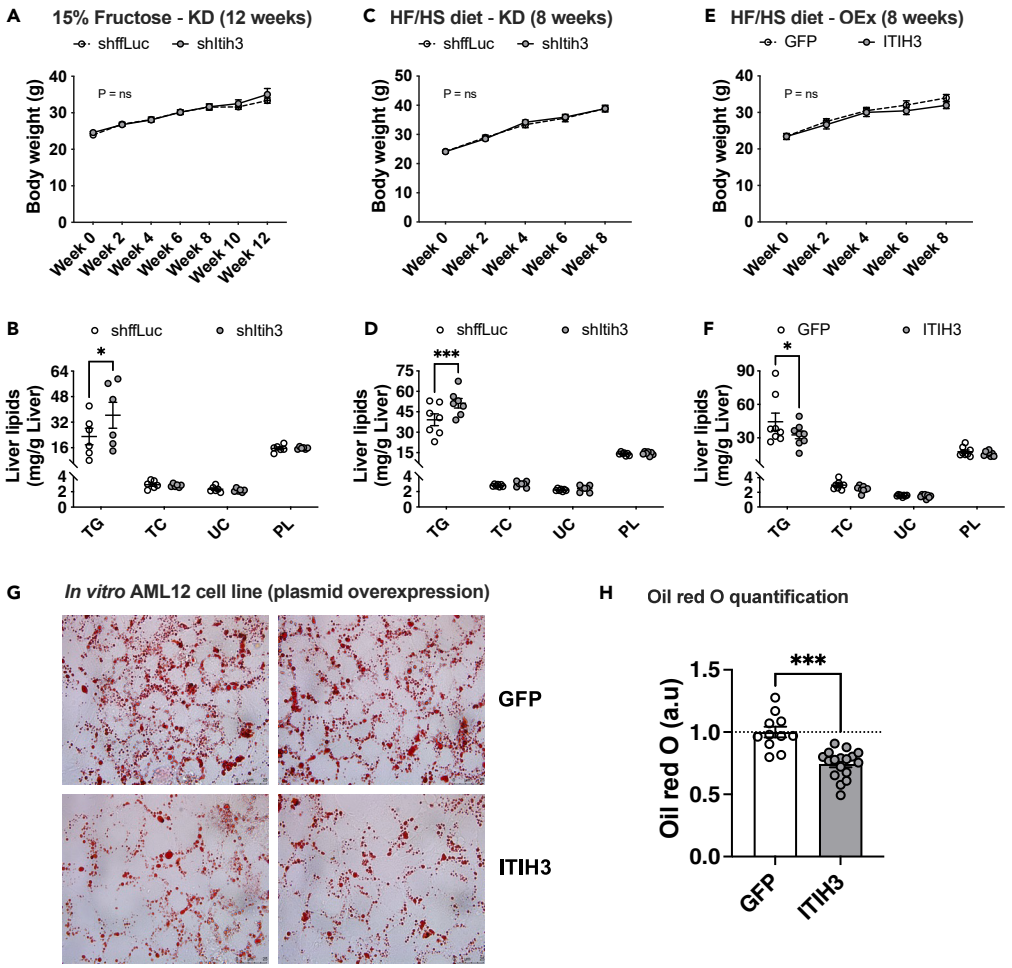

Figure 2. ITIH3 lowers liver triglyceride accumulation both *in vivo* and *in vitro*

Comparisons of body weight measurements and hepatic lipid levels from (A and B) 15% fructose in drinking water or (C and D) HF/HS fed ITIH3 silencing (KD) mice or (E and F) HF/HS fed ITIH3 overexpressing (OEx) mice, respectively. Oil Red O staining of AML12 cells overexpressing GFP or ITIH3 with (G) representative images and (H) quantification. Data are presented as mean ± SEM (n = 6–8 mice per group; *n* = 2 independent experiments for AML12 cells). *p* values were calculated by (A, C, and E) repeated measures two-factor ANOVA; (B, D, and F) two-factor ANOVA corrected by post-hoc "Holm-Sidak's" multiple comparisons test; (H) t test. *$p < 0.05$; ***$p < 0.001$. TG, triglyceride; TC, total cholesterol; UC, unesterified cholesterol; PL, phospholipids.

measured mitochondrial respiration capacities in both *in vivo* and *in vitro* conditions using XF Pro Seahorse bioanalyzer as described in the STAR methods section. First, we isolated liver mitochondria from HF/HS fed animals overexpressing either GFP or ITIH3. We observed that ITIH3 overexpression significantly reduced the mitochondrial respiration profile especially in the presence of complex II substrates (Figures 3A and 3B). Also, we noted that ITIH3 overexpression reduced complex II mediated mitochondrial respiration at both State 3 (ADP-stimulated) and State 3u (FCCP-stimulated) respiration (Figures 3C and 3D).

To further address the role of ITIH3 *in vitro*, AML12 liver cells overexpressing GFP or ITIH3 for 48 h were used to measure cellular respiration using XF Pro Seahorse bioanalyzer. We observed that ITIH3 overexpression significantly reduced the cellular respiration profile (Figure 3E). Furthermore, individual measurements revealed that ITIH3 overexpression reduced mitochondrial, ATP-linked, maximal, and spare capacity related respiration (Figures 3F–3I). Since, ITIH3 is a secreted hepatokine, we next treated the AML12 liver cells with recombinant human ITIH3 protein (rhITIH3) for 24 h and repeated our cellular bioenergetic experiments to corroborate these results. As expected, we observed significantly reduced cellular respiration profile and corresponding individual measurements only in the rhITIH3 treated cells (Figures 3J–3N). Altogether, we conclude that ITIH3 confers hepatoprotection against steatosis by lowering mitochondrial respiration.

ITIH3 protects against steatosis by downregulating mitochondria and *de novo* lipogenesis genes while upregulating *Stat3* expression and STAT1 signaling

To further explore the mechanistic roles of ITIH3 in the observed metabolic alterations, we performed whole genome RNA sequencing on the extracted liver tissues from ITIH3 overexpression groups. We found 480 differentially expressed genes (DEGs) in ITIH3 overexpression animals

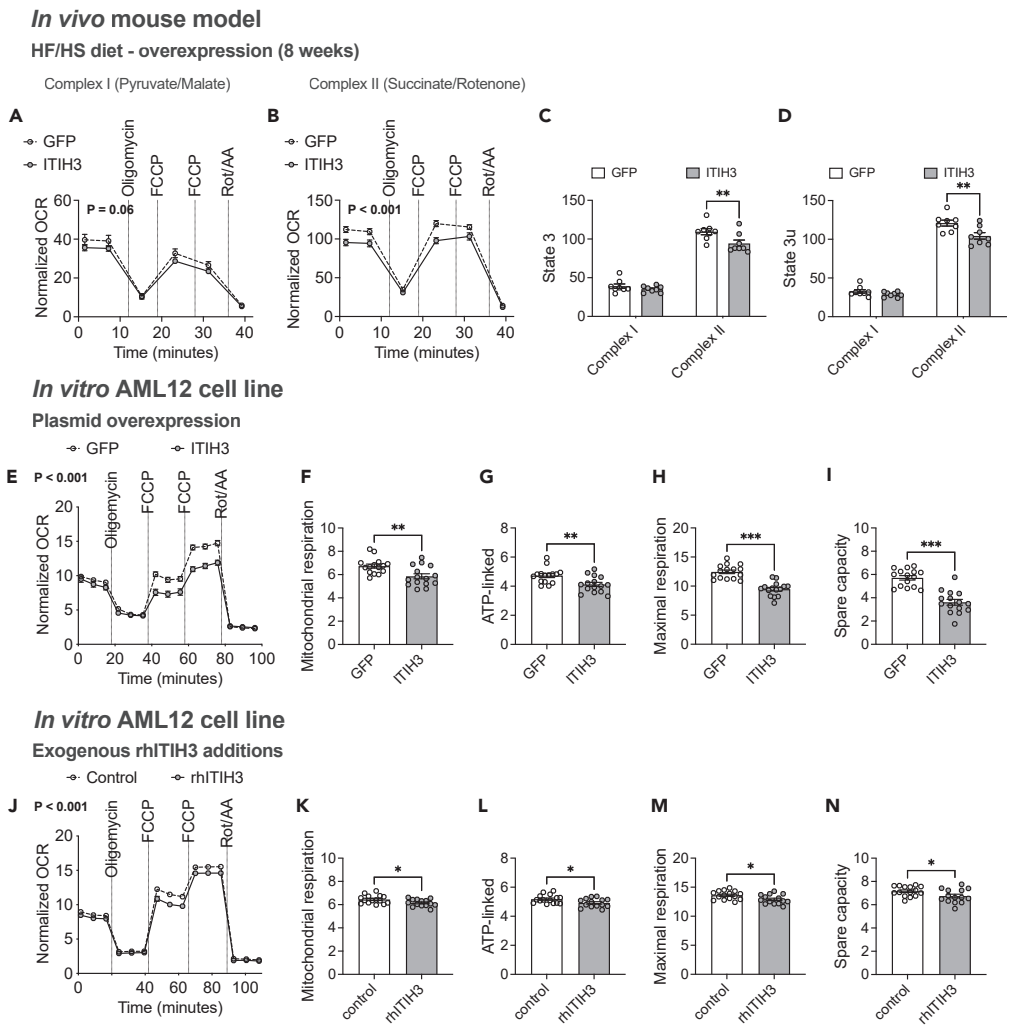

Figure 3. ITIH3 lowers mitochondrial respiration both *in vivo* and *in vitro*

Respirometry traces of isolated liver mitochondria from GFP or ITIH3 overexpressing mice offered (A) pyruvate with malate (Complex I) or (B) succinate with rotenone (Complex II) and their respective (C) State 3 and (D) State 3u mitochondrial respiration. Respirometry traces of intact AML12 cells (E) overexpressing GFP or ITIH3, or (J) exogenously treated with control or rhITIH3 and their respective (F and K) mitochondrial (datapoint 15 subtracted from 3), (G and L) ATP-linked (datapoint 6 subtracted from 3), (H and M) maximal respiration (datapoint 15 subtracted from 12) and (I and N) spare capacity (datapoint 3 subtracted from 12), respectively. Data are presented as mean ± SEM (n = 8 mice per group; n = 14–15 replicates per group for AML12 cells). p values were calculated by (A, B, E and J) repeated measures two-factor ANOVA; (C and D) multiple t tests corrected by post-hoc 'Holm-Sidak's' multiple comparisons test; (F–I and K–N) t test. *$p < 0.05$; **$p < 0.01$; ***$p < 0.001$.

(Figure 4A; Table S2). Key NAFLD/NASH genes that were significantly changed in ITIH3 overexpression groups include *Dgat2*, *Mpc2*, and *Stat1*. Notably, both DGAT2[45–47] and MPC2[48–50] are considered as promising drug targets against NAFLD/NASH and were both downregulated in ITIH3 overexpression mice. On the other hand, STAT1, which plays an essential role in response to interferons, was reported to inhibit both liver mitochondrial biogenesis[51] and liver fibrosis[52,53] and was found to be upregulated in ITIH3 overexpression. Follow-up network enrichment analyses of the 480 DEGs by DAVID[41] revealed NAFLD-related metabolic pathways such as mitochondria, fatty acid metabolism, organic acid metabolism, and retinol metabolism (Figure 4B). Interestingly, interferon signaling pathways were also enriched. Furthermore, gene set enrichment analysis (GSEA) of ranked DEGs identified mitochondria as a downregulated gene set (Enrichment score: −0.452, p = 3.89E-07) and response to Type I interferon as an upregulated gene set (Enrichment score: 0.615, p = 7.31E-04) (Figures 4C and 4D).

It has been proposed that hepatic DNL is elevated in NAFLD, which is one of the central reasons for accumulation of hepatic lipids.[54] Furthermore, since our bioenergetic analyses revealed that ITIH3 negatively affects mitochondrial respiration capacity (Figure 3), we reasoned that reduced mitochondrial capacity implies reduced TCA cycle flux and substrate (citrate) generation for DNL thus lowering it. To test this, we first investigated the expression of DNL genes in our *in vivo* liver samples. We observed that DNL-related genes such as *Fasn*, *Elovl6*, and *Scd1* were significantly elevated in ITIH3 silencing compared to shffLuc control animals (Figure 4E). In contrast, ITIH3 overexpression lowered the

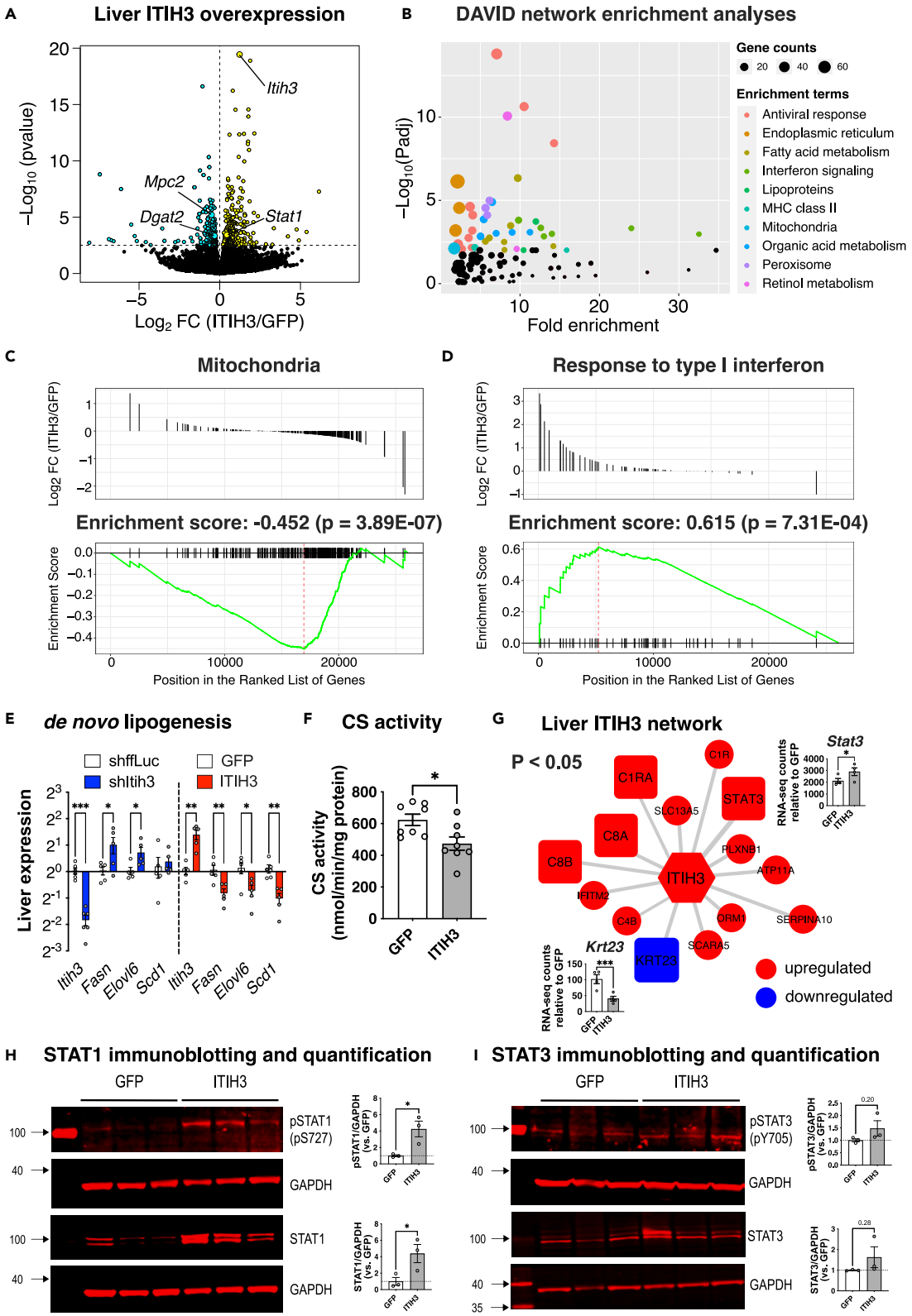
A
Liver ITIH3 overexpression
Itih3
Mpc2
Dgat2
Stat1
−Log10 (pvalue)
Log2 FC (ITIH3/GFP)
B
DAVID network enrichment analyses
Gene counts
20
40
60
Enrichment terms
Antiviral response
Endoplasmic reticulum
Fatty acid metabolism
Interferon signaling
Lipoproteins
MHC class II
Mitochondria
Organic acid metabolism
Peroxisome
Retinol metabolism
−Log10(Padj)
Fold enrichment
C
Mitochondria
Log2 FC (ITIH3/GFP)
Enrichment score: -0.452 (p = 3.89E-07)
Enrichment Score
Position in the Ranked List of Genes
D
Response to type I interferon
Log2 FC (ITIH3/GFP)
Enrichment score: 0.615 (p = 7.31E-04)
Enrichment Score
Position in the Ranked List of Genes
E
de novo lipogenesis
shffLuc
shItih3
GFP
ITIH3
Liver expression
Itih3
Fasn
Elovl6
Scd1
F
CS activity
CS activity (nmol/min/mg protein)
GFP
ITIH3
G
Liver ITIH3 network
P < 0.05
C1R
C1RA
STAT3
SLC13A5
C8A
C8B
PLXNB1
ITIH3
ATP11A
IFITM2
C4B
ORM1
SERPINA10
SCARA5
KRT23
Stat3
RNA-seq counts relative to GFP
Krt23
upregulated
downregulated
H
STAT1 immunoblotting and quantification
GFP
ITIH3
pSTAT1 (pS727)
GAPDH
STAT1
pSTAT1/GAPDH (vs. GFP)
I
STAT3 immunoblotting and quantification
pSTAT3 (pY705)
STAT3
pSTAT3/GAPDH (vs. GFP)

Figure 4. ITIH3 protects against steatosis via downregulating mitochondria and *de novo* lipogenesis while upregulating STAT1 signaling

(A) Global genome-wide transcriptomics of livers extracted from GFP or ITIH3 overexpressing mice. Turquoise and yellow represent down-regulated and up-regulated genes, respectively.

(B) DAVID pathway enrichment analyses of 480 DEGs (listed in Table S2). Gene set enrichment analysis (GSEA) of ranked DEGs revealed a significant enrichment of (C) Mitochondria and (D) Response to type I interferon. Follow-up (E) qPCR analyses of *Itih3* and liver DNL genes such as *Fasn*, *Elovl6*, and *Scd1* in ITIH3 knockdown and overexpression mice and their respective controls and (F) citrate synthase (CS) activity measured in GFP or ITIH3 overexpression mice.

(G) Overlay of DEGs on ITIH3 network from Figure 1A. Blue represents genes going down and red represents genes going up in ITIH3 overexpressing mice ($p < 0.05$). Inset shows RNA counts of *Stat3* and *Krt23* in ITIH3 overexpressing mice. Follow-up immunoblot analyses and their respective quantification of liver proteins such as (H) pSTAT1 and STAT1, (I) pSTAT3 and STAT3 in GFP or ITIH3 overexpressing mice. GAPDH was used as a loading control. Data are presented as mean ± SEM ($n = 4$ mice for transcriptomics, n = 5–6 mice for qPCR, $n = 8$ for CS activity and $n = 3$ mice for immunoblot analyses per group). *p* values were calculated by (A and G) Wald test; (E) multiple t tests corrected by post-hoc "Benjamini, Krieger, Yekutieli" FDR approach for multiple comparisons test; (F, H, and I) t test. $*p < 0.05$; $**p < 0.01$; $***p < 0.001$.

DNL-related genes compared to GFP control animals (Figure 4E). Furthermore, we observed that ITIH3 overexpression lowered TCA cycle flux as measured by citrate synthase (CS) activity (Figure 4F). Overall, this further highlights the importance of ITIH3 in conferring hepatoprotection against steatosis via lowering DNL. Next, when we reanalyzed the ITIH3 network (Figure 1A), we found that 13 genes were positively regulated including *Stat3* and complement factors and one gene (*Krt23*), a reported biomarker for NASH and HCC progression,[38] was negatively regulated in ITIH3 overexpression mice (Figure 4G). Finally, western blot analyses demonstrated that ITIH3 overexpression increased both activated STAT1 (phosphorylated STAT1, pSTAT1) and total STAT1 protein levels in the liver (Figure 4H). We also found an increased trend of both activated STAT3 (phosphorylated STAT3, pSTAT3) and total STAT3 liver protein levels in ITIH3 overexpression mice (Figure 4I). Further investigation into whether ITIH3 regulated STAT3 via IL-6/JAK pathway revealed us that ITIH3 overexpression had no effect on the levels of *Il1b*, *Il6*, *Socs3*, *Jak1* RNA, or JAK1 protein (Figure S7). Overall, ITIH3 overexpression studies demonstrated that hepatic ITIH3 negatively regulates DNL gene expression and mitochondria, while positively regulating *Stat3* expression and STAT1 signaling.

DISCUSSION

In this study, we demonstrate that hepatokine ITIH3 inversely regulates NAFLD pathology by providing multiple evidence ranging from population studies to *in vitro* and *in vivo* studies. Population studies using ~100 HMDP strains maintained on different diet conditions and 262 human liver biopsies revealed that hepatic *Itih3* expression was inversely associated with NAFLD progression and hepatic TG accumulation. ITIH3 loss- or gain-of-function studies in both animal and cell culture models revealed inverse relationship between ITIH3 and hepatic lipid content, mitochondrial respiration, and DNL. Altogether, our results reveal a hepatoprotective role of ITIH3 on NAFLD that is distinct from its known functions.

Inter-tissue crosstalk by endocrine factors or secretory proteins is conserved throughout evolution and is mediated by almost all organisms. As a result, many secretory proteins have been identified. Recent works utilizing "omics" technologies have enabled the identification of systemic regulators of whole-body homeostasis.[55,56] Previously, cell or tissue specific secretome have been studied by using various methodological approaches such as proteomic analysis of cell culture medium or by examining the transcriptome data for the presence of signal peptides.[57,58] Most importantly, inter-tissue communication was also addressed by analyzing plasma proteomics followed by candidate biomarker identification.[59,60] A recent work from Seldin et al. report the importance of novel endocrine factors responsible for inter-tissue communication.[61] Most notably, several secretory proteins based pharmacological agents such as GLP-1 receptor antagonists, FGF-19/21 analogs, and MOTS-c analogs are at different stages of clinical trials for NAFLD/NASH treatments.[62] Here, we report a hitherto unknown role of a hepatokine ITIH3 in NAFLD protection.

Liver is the central secretory organ of the human body; it secretes majority of the blood proteins that have profound impact in the systemic homeostasis. During liver abnormalities, liver enzymes in the circulation are routinely measured to diagnose the liver diseases. Remarkably, plasma protein profiling of type 2 diabetes, NAFLD and NASH cohort patients resulted in the identification of proteins regulating blood coagulation or fibrinolysis factors, carrier proteins that play an important role in cholesterol metabolism and proteins involved in immune system regulation and inflammation.[63] Several studies have also shown that hepatokines regulate inflammation, insulin resistance, type 2 diabetes, obesity, steatosis, NAFLD, and cancer.[16,19,21,64,65] Thus, it was imperative to investigate the role of hepatokines that directly contribute to NAFLD. To this end, our integrative multiomics approach using ~100 HMDP strains identified the hepatokine ITIH3 as a potential NAFLD candidate gene that was strongly associated with several complement and coagulation factors. Indeed, our DAVID and ToppGene enrichment analyses prioritized NAFLD related gene networks and pathways such as fatty acid metabolism, mitochondria, TCA cycle, dyslipidemia, metabolic syndrome, fatty liver, steatohepatitis, fibrosis, complement activation, coagulation, and fibrinolysis pathways with respect to hepatic *Itih3* expression. Finally, our follow-up *in vitro* and *in vivo* validation studies verified the hepatoprotective role of ITIH3 against steatosis. All these data demonstrate that the hepatokine ITIH3 could be employed as a biomarker or potential treatment for severe NAFLD/NASH pathologies. Nevertheless, future investigations involving comparative proteome analyses of liver and plasma are warranted to determine what extrinsic vs. intrinsic metabolic changes are mediated by ITIH3.

Several studies have shown that mitochondrial dysfunction is causal in developing NAFLD and its progression.[15,66] Despite the importance of hepatokines in NAFLD progression, little is known on the role of these proteins in mitochondrial function. Given that our DAVID enrichment prioritized the involvement of fatty acid metabolism, mitochondria, and TCA cycle with respect to ITIH3 and to further explore the mechanistic connections between ITIH3 and NAFLD, we focused on ITIH3's role in mitochondrial function. During the initial stages of NAFLD (hepatic

steatosis) there is an acute increase in the mitochondrial functions to combat the excessive nutrient availability and ATP demand resulting in a hyperactive OXPHOS phenotype.[15,43] Over time, this will result in elevated ROS generation which may lead to reduced mitochondrial function, thus progressing to severe stages of NAFLD, such as NASH and fibrosis.[43,66–68] Hyperactive OXPHOS will also lead to elevated TCA cycle flux resulting in augmented DNL thereby causing hepatic steatosis.[69] Indeed, we had earlier shown that lowering mitochondrial function will reduce DNL and hepatic steatosis.[15,44] In this study, both our *in vitro* and *in vivo* experiments confirmed that ITIH3 reduced the mitochondrial functions that were elevated during steatosis. Our findings thus emphasize ITIH3's role as a regulator of mitochondrial function.

Several factors are known to contribute to the intrahepatic lipid accumulation during hepatic steatosis such as elevated hepatic free fatty acid uptake coming from the diet or adipose tissue lipolysis, augmented DNL, reduced fatty acid oxidation and reduced VLDL secretion. Nevertheless, a large number of studies have demonstrated the upregulation and the causal effects of DNL genes such as *Fasn*, *Elovl6*, and *Scd1* during NAFLD.[70–72] Furthermore, both animal and human studies have demonstrated that DNL is a distinguishing feature of NAFLD.[54,73–76] Indeed, our *in vivo* studies demonstrated that ITIH3 knockdown increased DNL genes such as *Fasn*, *Elovl6*, and *Scd1*, while ITIH3 overexpression downregulated them. Similarly, ITIH3 overexpression reduced TCA cycle flux. Thus, our results corroborate with previous literature as well as highlight the importance of ITIH3 as a negative regulator of liver DNL.

Finally, we wanted to gain a clear mechanistic understanding of how the hepatokine ITIH3 exerts its hepatoprotective functions. Our network modeling analyses gave us a clue in which we observed that STAT3 was directly connected to ITIH3 and positively correlated with hepatic *Itih3* expression. Accumulating evidence suggested that phosphorylated STAT3 translocate into the nucleus to activate the transcription of anti-steatosis and anti-fibrosis related genes.[33–35,77] Additionally, we observed strong positive correlation between expression of *ITIH3* and *STAT3* in our human NAFLD cohort (bicor = 4.2, p = 7.1E-13). We therefore speculated that ITIH3 works via STAT3 to ameliorate NAFLD. Indeed, our global gene expression analyses revealed us that liver *Stat3* expression was high in ITIH3 overexpressing mice but immunoblot analyses revealed only an increased trend. Surprisingly, we also observed that ITIH3 overexpression significantly upregulated liver STAT1 at both the RNA and protein levels, as well as activation (pSTAT1-pS727). Indeed, STAT1 has been validated by others to inhibit both liver mitochondrial biogenesis via negatively regulating *Pgc1α*[51] and liver fibrosis via negatively regulating TGF-β signaling.[52,53] Based on these findings, we suspect that ITIH3 functions through STAT1 and possibly STAT3 signaling, although further studies are required to confirm this.

In conclusion, our study demonstrated that the hepatokine ITIH3 plays a unique role in controlling hepatic lipid profile, mitochondrial metabolism, and DNL, all of which have implications for NAFLD treatment. We have also identified two potential pathways, STAT1 and STAT3, which may contribute to the observed hepatoprotection in ITIH3 overexpression.

Limitations of the study

Although our research addresses a potential mechanism of action for ITIH3 regarding mitochondrial metabolism and DNL via STAT1 and/or STAT3, the exact signaling sequences warrant additional investigation. Furthermore, although our hypothesis was formulated using mouse and human population, all validation studies were performed using mice or murine cell lines. Finally, our current study does not investigate the potential role of ITIH3 in mitigating hepatic steatosis in female sex.

STAR★METHODS

Detailed methods are provided in the online version of this paper and include the following:

SUPPLEMENTAL INFORMATION

Supplemental information can be found online at https://doi.org/10.1016/j.isci.2024.109709.

ACKNOWLEDGMENTS

We thank Sarada Charugundla for liver lipid analyses; Anidya Soni, Meghan Curran, Dharshini Kumar, Zhiqiang Zhou, and Yonghong Meng for assistance in animal experiments. We acknowledge CSC–IT Center for Science, Finland, for computational resources. The graphical abstract was created with BioRender.com.

This work was supported by NIH R00DK120875 (K.C.K). The funders had no role in study design, data collection and interpretation, or the decision to submit the work for publication.

AUTHOR CONTRIBUTIONS

K.C.K. conceived the study. K.C.K., N.K.T., and U.M. designed, performed experiments, or analyzed the data. I.S.R., and A.P.R. performed cell culture experiments. M.P. cloned and constructed the AAV vectors. D.K., P.P., and J.P. collected, analyzed, or prepared the figures for the KOBS cohort data. K.C.K. and N.KT. drafted the manuscript, and all authors read or revised the manuscript.

DECLARATION OF INTERESTS

The authors declare no conflict of interests.

Received: October 30, 2023
Revised: February 16, 2024
Accepted: April 6, 2024
Published: April 10, 2024

REFERENCES

1. Adams, L.A., Lymp, J.F., St Sauver, J., Sanderson, S.O., Lindor, K.D., Feldstein, A., and Angulo, P. (2005). The natural history of nonalcoholic fatty liver disease: a population-based cohort study. Gastroenterology *129*, 113–121. https://doi.org/10.1053/j.gastro.2005.04.014.
2. Browning, J.D., Szczepaniak, L.S., Dobbins, R., Nuremberg, P., Horton, J.D., Cohen, J.C., Grundy, S.M., and Hobbs, H.H. (2004). Prevalence of hepatic steatosis in an urban population in the United States: impact of ethnicity. Hepatology *40*, 1387–1395. https://doi.org/10.1002/hep.20466.
3. Kopec, K.L., and Burns, D. (2011). Nonalcoholic fatty liver disease: a review of the spectrum of disease, diagnosis, and therapy. Nutr. Clin. Pract. *26*, 565–576. https://doi.org/10.1177/0884533611419668.
4. Clark, J.M., Brancati, F.L., and Diehl, A.M. (2002). Nonalcoholic fatty liver disease. Gastroenterology *122*, 1649–1657. https://doi.org/10.1053/gast.2002.33573.
5. Falck-Ytter, Y., Younossi, Z.M., Marchesini, G., and McCullough, A.J. (2001). Clinical features and natural history of nonalcoholic steatosis syndromes. Semin. Liver Dis. *21*, 17–26. https://doi.org/10.1055/s-2001-12926.
6. Marchesini, G., Bugianesi, E., Forlani, G., Cerrelli, F., Lenzi, M., Manini, R., Natale, S., Vanni, E., Villanova, N., Melchionda, N., and Rizzetto, M. (2003). Nonalcoholic fatty liver, steatohepatitis, and the metabolic syndrome. Hepatology *37*, 917–923. https://doi.org/10.1053/jhep.2003.50161.
7. Pan, J.J., and Fallon, M.B. (2014). Gender and racial differences in nonalcoholic fatty liver disease. World J. Hepatol. *6*, 274–283. https://doi.org/10.4254/wjh.v6.i5.274.
8. Ruhl, C.E., and Everhart, J.E. (2003). Determinants of the association of overweight with elevated serum alanine aminotransferase activity in the United States. Gastroenterology *124*, 71–79. https://doi.org/10.1053/gast.2003.50004.
9. Clark, J.M., Brancati, F.L., and Diehl, A.M. (2003). The prevalence and etiology of elevated aminotransferase levels in the United States. Am. J. Gastroenterol. *98*, 960–967. https://doi.org/10.1111/j.1572-0241.2003.07486.x.
10. Ioannou, G.N., Boyko, E.J., and Lee, S.P. (2006). The prevalence and predictors of elevated serum aminotransferase activity in the United States in 1999-2002. Am. J. Gastroenterol. *101*, 76–82. https://doi.org/10.1111/j.1572-0241.2005.00341.x.
11. Lazo, M., Hernaez, R., Eberhardt, M.S., Bonekamp, S., Kamel, I., Guallar, E., Koteish, A., Brancati, F.L., and Clark, J.M. (2013). Prevalence of nonalcoholic fatty liver disease in the United States: the Third National Health and Nutrition Examination Survey, 1988-1994. Am. J. Epidemiol. *178*, 38–45. https://doi.org/10.1093/aje/kws448.
12. Schneider, A.L.C., Lazo, M., Selvin, E., and Clark, J.M. (2014). Racial differences in nonalcoholic fatty liver disease in the U.S. population. Obesity *22*, 292–299. https://doi.org/10.1002/oby.20426.
13. de Alwis, N.M.W., and Day, C.P. (2008). Non-alcoholic fatty liver disease: the mist gradually clears. J. Hepatol. *48*, S104–S112. https://doi.org/10.1016/j.jhep.2008.01.009.
14. McCullough, A.J. (2004). The clinical features, diagnosis and natural history of nonalcoholic fatty liver disease. Clin. Liver Dis. *8*, 521–533. https://doi.org/10.1016/j.cld.2004.04.004.
15. Chella Krishnan, K., Kurt, Z., Barrere-Cain, R., Sabir, S., Das, A., Floyd, R., Vergnes, L., Zhao, Y., Che, N., Charugundla, S., et al. (2018). Integration of Multi-omics Data from Mouse Diversity Panel Highlights Mitochondrial Dysfunction in Non-alcoholic Fatty Liver Disease. Cell Syst. *6*, 103–115.e7. https://doi.org/10.1016/j.cels.2017.12.006.
16. Misu, H., Takamura, T., Matsuzawa, N., Shimizu, A., Ota, T., Sakurai, M., Ando, H., Arai, K., Yamashita, T., Honda, M., et al. (2007). Genes involved in oxidative phosphorylation are coordinately upregulated with fasting hyperglycaemia in livers of patients with type 2 diabetes. Diabetologia *50*, 268–277. https://doi.org/10.1007/s00125-006-0489-8.
17. Takamura, T., Sakurai, M., Ota, T., Ando, H., Honda, M., and Kaneko, S. (2004). Genes for systemic vascular complications are differentially expressed in the livers of type 2 diabetic patients. Diabetologia *47*, 638–647. https://doi.org/10.1007/s00125-004-1366-y.
18. Takeshita, Y., Takamura, T., Hamaguchi, E., Shimizu, A., Ota, T., Sakurai, M., and Kaneko, S. (2006). Tumor necrosis factor-alpha-induced production of plasminogen activator inhibitor 1 and its regulation by pioglitazone and cerivastatin in a nonmalignant human hepatocyte cell line. Metabolism *55*, 1464–1472. https://doi.org/10.1016/j.metabol.2006.06.016.
19. Meex, R.C., Hoy, A.J., Morris, A., Brown, R.D., Lo, J.C.Y., Burke, M., Goode, R.J.A., Kingwell, B.A., Kraakman, M.J., Febbraio, M.A., et al. (2015). Fetuin B Is a Secreted Hepatocyte Factor Linking Steatosis to Impaired Glucose Metabolism. Cell Metabol. *22*, 1078–1089. https://doi.org/10.1016/j.cmet.2015.09.023 PMID - 26603189.
20. Vernia, S., Cavanagh-Kyros, J., Garcia-Haro, L., Sabio, G., Barrett, T., Jung, D.Y., Kim, J.K., Xu, J., Shulha, H.P., Garber, M., et al. (2014). The PPARalpha-FGF21 hormone axis contributes to metabolic regulation by the hepatic JNK signaling pathway. Cell Metabol. *20*, 512–525. https://doi.org/10.1016/j.cmet.2014.06.010.

21. Misu, H., Takamura, T., Takayama, H., Hayashi, H., Matsuzawa-Nagata, N., Kurita, S., Ishikura, K., Ando, H., Takeshita, Y., Ota, T., et al. (2010). A liver-derived secretory protein, selenoprotein P, causes insulin resistance. Cell Metabol. *12*, 483–495. https://doi.org/10.1016/j.cmet.2010.09.015.
22. Bourguignon, J., Vercaigne, D., Sesboüé, R., Martin, J.P., and Salier, J.P. (1983). Inter-alpha-trypsin-inhibitor (ITI): two distinct mRNAs in baboon liver argue for a discrete synthesis of ITI and ITI derivatives. FEBS Lett. *162*, 379–383. https://doi.org/10.1016/0014-5793(83)80791-1.
23. Bost, F., Diarra-Mehrpour, M., and Martin, J.P. (1998). Inter-alpha-trypsin inhibitor proteoglycan family–a group of proteins binding and stabilizing the extracellular matrix. Eur. J. Biochem. *252*, 339–346. https://doi.org/10.1046/j.1432-1327.1998.2520339.x.
24. Chen, L., Mao, S.J., McLean, L.R., Powers, R.W., and Larsen, W.J. (1994). Proteins of the inter-alpha-trypsin inhibitor family stabilize the cumulus extracellular matrix through their direct binding with hyaluronic acid. J. Biol. Chem. *269*, 28282–28287.
25. Fries, E., and Kaczmarczyk, A. (2003). Inter-alpha-inhibitor, hyaluronan and inflammation. Acta Biochim. Pol. *50*, 735–742.
26. Kobayashi, H., Shinohara, H., Ohi, H., Sugimura, M., Terao, T., and Fujie, M. (1994). Urinary trypsin inhibitor (UTI) and fragments derived from UTI by limited proteolysis efficiently inhibit tumor cell invasion. Clin. Exp. Metastasis *12*, 117–128. https://doi.org/10.1007/BF01753978.
27. Schreitmüller, T., Hochstrasser, K., Reisinger, P.W., Wachter, E., and Gebhard, W. (1987). cDNA cloning of human inter-alpha-trypsin inhibitor discloses three different proteins. Biol. Chem. Hoppe Seyler *368*, 963–970. https://doi.org/10.1515/bchm3.1987.368.2.963.
28. Gomis-Rüth, F.X., Maskos, K., Betz, M., Bergner, A., Huber, R., Suzuki, K., Yoshida, N., Nagase, H., Brew, K., Bourenkov, G.P., et al. (1997). Mechanism of inhibition of the human matrix metalloproteinase stromelysin-1 by TIMP-1. Nature *389*, 77–81. https://doi.org/10.1038/37995.
29. Ossowski, L. (1988). Plasminogen activator dependent pathways inthe dissemination of human tumor cells in the chick embryo. Cell *52*, 321–328. https://doi.org/10.1016/s0092-8674(88)80025-4.
30. Kim, T.H., Koo, J.H., Heo, M.J., Han, C.Y., Kim, Y.I., Park, S.Y., Cho, I.J., Lee, C.H., Choi, C.S., Lee, J.W., et al. (2019). Overproduction of inter-alpha-trypsin inhibitor heavy chain 1 after loss of Galpha(13) in liver exacerbates systemic insulin resistance in mice. Sci. Transl. Med. *11*, eaan4735. https://doi.org/10.1126/scitranslmed.aan4735.
31. Nakamura, N., Hatano, E., Iguchi, K., Sato, M., Kawaguchi, H., Ohtsu, I., Sakurai, T., Aizawa, N., Iijima, H., Nishiguchi, S., et al. (2019). Elevated levels of circulating ITIH4 are associated with hepatocellular carcinoma with nonalcoholic fatty liver disease: from pig model to human study. BMC Cancer *19*, 621. https://doi.org/10.1186/s12885-019-5825-8.
32. Lai, K.K.Y., Kolippakkam, D., and Beretta, L. (2008). Comprehensive and quantitative proteome profiling of the mouse liver and plasma. Hepatology *47*, 1043–1051. https://doi.org/10.1002/hep.22123.
33. Wang, H., Lafdil, F., Kong, X., and Gao, B. (2011). Signal transducer and activator of transcription 3 in liver diseases: a novel therapeutic target. Int. J. Biol. Sci. *7*, 536–550. https://doi.org/10.7150/ijbs.7.536.
34. Ki, S.H., Park, O., Zheng, M., Morales-Ibanez, O., Kolls, J.K., Bataller, R., and Gao, B. (2010). Interleukin-22 treatment ameliorates alcoholic liver injury in a murine model of chronic-binge ethanol feeding: role of signal transducer and activator of transcription 3. Hepatology *52*, 1291–1300. https://doi.org/10.1002/hep.23837.
35. Yang, L., Zhang, Y., Wang, L., Fan, F., Zhu, L., Li, Z., Ruan, X., Huang, H., Wang, Z., Huang, Z., et al. (2010). Amelioration of high fat diet induced liver lipogenesis and hepatic steatosis by interleukin-22. J. Hepatol. *53*, 339–347. https://doi.org/10.1016/j.jhep.2010.03.004.
36. Xu, L., Han, J., Yang, Z.H.E., Yang, Y., Chen, J., Wu, X., Hong, Y.A.N., and Wang, Q.I. (2022). Lrg1 Inhibits the Activation of Hepatic Macrophages to Alleviate NAFLD by Enhancing TGF-B1 Signaling. https://doi.org/10.21203/rs.3.rs-1440311/v2.
37. Zhang, X., Shen, J., Man, K., Chu, E.S.H., Yau, T.O., Sung, J.C.Y., Go, M.Y.Y., Deng, J., Lu, L., Wong, V.W.S., et al. (2014). CXCL10 plays a key role as an inflammatory mediator and a non-invasive biomarker of non-alcoholic steatohepatitis. J. Hepatol. *61*, 1365–1375. https://doi.org/10.1016/j.jhep.2014.07.006 PMID - 25048951.
38. Starmann, J., Fälth, M., Spindelböck, W., Lanz, K.L., Lackner, C., Zatloukal, K., Trauner, M., and Sültmann, H. (2012). Gene expression profiling unravels cancer-related hepatic molecular signatures in steatohepatitis but not in steatosis. PLoS One *7*, e46584. https://doi.org/10.1371/journal.pone.0046584.
39. Hui, S.T., Parks, B.W., Org, E., Norheim, F., Che, N., Pan, C., Castellani, L.W., Charugundla, S., Dirks, D.L., Psychogios, N., et al. (2015). The genetic architecture of NAFLD among inbred strains of mice. Elife *4*, e05607. https://doi.org/10.7554/eLife.05607 PMID - 26067236.
40. Hui, S.T., Kurt, Z., Tuominen, I., Norheim, F., C Davis, R., Pan, C., Dirks, D.L., Magyar, C.E., French, S.W., Chella Krishnan, K., et al. (2018). The Genetic Architecture of Diet-Induced Hepatic Fibrosis in Mice. Hepatology *68*, 2182–2196. https://doi.org/10.1002/hep.30113.
41. Huang, D.W., Sherman, B.T., and Lempicki, R.A. (2008). Systematic and integrative analysis of large gene lists using DAVID bioinformatics resources. Nat. Protoc. *4*, 44–57. https://doi.org/10.1038/nprot.2008.211 PMID - 19131956.
42. Chen, J., Bardes, E.E., Aronow, B.J., and Jegga, A.G. (2009). ToppGene Suite for gene list enrichment analysis and candidate gene prioritization. Nucleic Acids Res. *37*, W305–W311. https://doi.org/10.1093/nar/gkp427.
43. Shum, M., Ngo, J., Shirihai, O.S., and Liesa, M. (2021). Mitochondrial oxidative function in NAFLD: Friend or foe? Mol. Metabol. *50*, 101134. https://doi.org/10.1016/j.molmet.2020.101134.
44. Chella Krishnan, K., Floyd, R.R., Sabir, S., Jayasekera, D.W., Leon-Mimila, P.V., Jones, A.E., Cortez, A.A., Shravah, V., Péterfy, M., Stiles, L., et al. (2021). Liver Pyruvate Kinase Promotes NAFLD/NASH in Both Mice and Humans in a Sex-Specific Manner. Cell. Mol. Gastroenterol. Hepatol. *11*, 389–406. https://doi.org/10.1016/j.jcmgh.2020.09.004.
45. Gluchowski, N.L., Gabriel, K.R., Chitraju, C., Bronson, R.T., Mejhert, N., Boland, S., Wang, K., Lai, Z.W., Farese, R.V., Jr., and Walther, T.C. (2019). Hepatocyte Deletion of Triglyceride-Synthesis Enzyme Acyl CoA: Diacylglycerol Acyltransferase 2 Reduces Steatosis Without Increasing Inflammation or Fibrosis in Mice. Hepatology *70*, 1972–1985. https://doi.org/10.1002/hep.30765.
46. Calle, R.A., Amin, N.B., Carvajal-Gonzalez, S., Ross, T.T., Bergman, A., Aggarwal, S., Crowley, C., Rinaldi, A., Mancuso, J., Aggarwal, N., et al. (2021). ACC inhibitor alone or co-administered with a DGAT2 inhibitor in patients with non-alcoholic fatty liver disease: two parallel, placebo-controlled, randomized phase 2a trials. Nat. Med. *27*, 1836–1848. https://doi.org/10.1038/s41591-021-01489-1.
47. Yenilmez, B., Wetoska, N., Kelly, M., Echeverria, D., Min, K., Lifshitz, L., Alterman, J.F., Hassler, M.R., Hildebrand, S., DiMarzio, C., et al. (2022). An RNAi therapeutic targeting hepatic DGAT2 in a genetically obese mouse model of nonalcoholic steatohepatitis. Mol. Ther. *30*, 1329–1342. https://doi.org/10.1016/j.ymthe.2021.11.007.
48. McCommis, K.S., Hodges, W.T., Brunt, E.M., Nalbantoglu, I., McDonald, W.G., Holley, C., Fujiwara, H., Schaffer, J.E., Colca, J.R., and Finck, B.N. (2017). Targeting the mitochondrial pyruvate carrier attenuates fibrosis in a mouse model of nonalcoholic steatohepatitis. Hepatology *65*, 1543–1556. https://doi.org/10.1002/hep.29025.
49. Habibi, M., Ferguson, D., Eichler, S.J., Chan, M.M., LaPoint, A., Shew, T.M., He, M., Lutkewitte, A.J., Schilling, J.D., Cho, K.Y., et al. (2023). Mitochondrial Pyruvate Carrier Inhibition Attenuates Hepatic Stellate Cell Activation and Liver Injury in a Mouse Model of Metabolic Dysfunction-associated Steatotic Liver Disease. Preprint at bioRxiv. https://doi.org/10.1101/2023.02.13.528384.
50. McCommis, K.S., Chen, Z., Fu, X., McDonald, W.G., Colca, J.R., Kletzien, R.F., Burgess, S.C., and Finck, B.N. (2015). Loss of Mitochondrial Pyruvate Carrier 2 in the Liver Leads to Defects in Gluconeogenesis and Compensation via Pyruvate-Alanine Cycling. Cell Metabol. *22*, 682–694. https://doi.org/10.1016/j.cmet.2015.07.028.
51. Sisler, J.D., Morgan, M., Raje, V., Grande, R.C., Derecka, M., Meier, J., Cantwell, M., Szczepanek, K., Korzun, W.J., Lesnefsky, E.J., et al. (2015). The Signal Transducer and Activator of Transcription 1 (STAT1) Inhibits Mitochondrial Biogenesis in Liver and Fatty Acid Oxidation in Adipocytes. PLoS One *10*, e0144444. https://doi.org/10.1371/journal.pone.0144444.
52. Jeong, W.I., Park, O., Radaeva, S., and Gao, B. (2006). STAT1 inhibits liver fibrosis in mice by inhibiting stellate cell proliferation and stimulating NK cell cytotoxicity. Hepatology *44*, 1441–1451. https://doi.org/10.1002/hep.21419.
53. Martí-Rodrigo, A., Alegre, F., Moragrega, Á.B., García-García, F., Martí-Rodrigo, P., Fernández-Iglesias, A., Gracia-Sancho, J., Apostolova, N., Esplugues, J.V., and Blas-García, A. (2020). Rilpivirine attenuates liver fibrosis through selective STAT1-mediated apoptosis in hepatic stellate cells. Gut *69*, 920–932. https://doi.org/10.1136/gutjnl-2019-318372.
54. Lambert, J.E., Ramos–Roman, M.A., Browning, J.D., and Parks, E.J. (2014). Increased De Novo Lipogenesis Is a Distinct Characteristic of Individuals With Nonalcoholic Fatty Liver Disease. Gastroenterology *146*, 726–735. https://doi.org/10.1053/j.gastro.2013.11.049.

55. Gehlenborg, N., O'Donoghue, S.I., Baliga, N.S., Goesmann, A., Hibbs, M.A., Kitano, H., Kohlbacher, O., Neuweger, H., Schneider, R., Tenenbaum, D., and Gavin, A.C. (2010). Visualization of omics data for systems biology. Nat. Methods *7*, S56–S68. https://doi.org/10.1038/nmeth.1436.
56. Civelek, M., and Lusis, A.J. (2014). Systems genetics approaches to understand complex traits. Nat. Rev. Genet. *15*, 34–48. https://doi.org/10.1038/nrg3575.
57. Hathout, Y. (2007). Approaches to the study of the cell secretome. Expert Rev. Proteomics *4*, 239–248. https://doi.org/10.1586/14789450.4.2.239.
58. Alvarez-Llamas, G., Szalowska, E., de Vries, M.P., Weening, D., Landman, K., Hoek, A., Wolffenbuttel, B.H.R., Roelofsen, H., and Vonk, R.J. (2007). Characterization of the human visceral adipose tissue secretome. Mol. Cell. Proteomics *6*, 589–600. https://doi.org/10.1074/mcp.M600265-MCP200.
59. Makridakis, M., and Vlahou, A. (2010). Secretome proteomics for discovery of cancer biomarkers. J. Proteonomics *73*, 2291–2305. https://doi.org/10.1016/j.jprot.2010.07.001.
60. Lawlor, K., Nazarian, A., Lacomis, L., Tempst, P., and Villanueva, J. (2009). Pathway-based biomarker search by high-throughput proteomics profiling of secretomes. J. Proteome Res. *8*, 1489–1503. https://doi.org/10.1021/pr8008572.
61. Seldin, M.M., Koplev, S., Rajbhandari, P., Vergnes, L., Rosenberg, G.M., Meng, Y., Pan, C., Phuong, T.M.N., Gharakhanian, R., Che, N., et al. (2018). A Strategy for Discovery of Endocrine Interactions with Application to Whole-Body Metabolism. Cell Metabol. *27*, 1138–1155.e6. https://doi.org/10.1016/j.cmet.2018.03.015.
62. Kim, K., and Kim, K.H. (2020). Targeting of Secretory Proteins as a Therapeutic Strategy for Treatment of Nonalcoholic Steatohepatitis (NASH). Int. J. Mol. Sci. *21*, 2296. https://doi.org/10.3390/ijms21072296 PMID - 32225108.
63. Niu, L., Geyer, P.E., Wewer Albrechtsen, N.J., Gluud, L.L., Santos, A., Doll, S., Treit, P.V., Holst, J.J., Knop, F.K., Vilsbøll, T., et al. (2019). Plasma proteome profiling discovers novel proteins associated with non-alcoholic fatty liver disease. Mol. Syst. Biol. *15*, e8793. https://doi.org/10.15252/msb.20188793.
64. Choi, J.W., Wang, X., Joo, J.I., Kim, D.H., Oh, T.S., Choi, D.K., and Yun, J.W. (2010). Plasma proteome analysis in diet-induced obesity-prone and obesity-resistant rats. Proteomics *10*, 4386–4400. https://doi.org/10.1002/pmic.201000391.
65. Oike, Y., Akao, M., Yasunaga, K., Yamauchi, T., Morisada, T., Ito, Y., Urano, T., Kimura, Y., Kubota, Y., Maekawa, H., et al. (2005). Angiopoietin-related growth factor antagonizes obesity and insulin resistance. Nat. Med. *11*, 400–408. https://doi.org/10.1038/nm1214.
66. Pessayre, D., and Fromenty, B. (2005). NASH: a mitochondrial disease. J. Hepatol. *42*, 928–940. https://doi.org/10.1016/j.jhep.2005.03.004.
67. Begriche, K., Igoudjil, A., Pessayre, D., and Fromenty, B. (2006). Mitochondrial dysfunction in NASH: causes, consequences and possible means to prevent it. Mitochondrion *6*, 1–28. https://doi.org/10.1016/j.mito.2005.10.004.
68. Begriche, K., Massart, J., Robin, M.A., Bonnet, F., and Fromenty, B. (2013). Mitochondrial adaptations and dysfunctions in nonalcoholic fatty liver disease. Hepatology *58*, 1497–1507. https://doi.org/10.1002/hep.26226.
69. Sunny, N.E., Parks, E.J., Browning, J.D., and Burgess, S.C. (2011). Excessive hepatic mitochondrial TCA cycle and gluconeogenesis in humans with nonalcoholic fatty liver disease. Cell Metabol. *14*, 804–810. https://doi.org/10.1016/j.cmet.2011.11.004.
70. Kotronen, A., Seppänen-Laakso, T., Westerbacka, J., Kiviluoto, T., Arola, J., Ruskeepää, A.L., Oresic, M., and Yki-Järvinen, H. (2009). Hepatic stearoyl-CoA desaturase (SCD)-1 activity and diacylglycerol but not ceramide concentrations are increased in the nonalcoholic human fatty liver. Diabetes *58*, 203–208. https://doi.org/10.2337/db08-1074.
71. Matsuzaka, T., Atsumi, A., Matsumori, R., Nie, T., Shinozaki, H., Suzuki-Kemuriyama, N., Kuba, M., Nakagawa, Y., Ishii, K., Shimada, M., et al. (2012). Elovl6 promotes nonalcoholic steatohepatitis. Hepatology *56*, 2199–2208. https://doi.org/10.1002/hep.25932.
72. Dorn, C., Riener, M.O., Kirovski, G., Saugspier, M., Steib, K., Weiss, T.S., Gäbele, E., Kristiansen, G., Hartmann, A., and Hellerbrand, C. (2010). Expression of fatty acid synthase in nonalcoholic fatty liver disease. Int. J. Clin. Exp. Pathol. *3*, 505–514.
73. Ferré, P., and Foufelle, F. (2010). Hepatic steatosis: a role for de novo lipogenesis and the transcription factor SREBP-1c. Diabetes Obes. Metabol. *12*, 83–92. https://doi.org/10.1111/j.1463-1326.2010.01275.x.
74. Belew, G.D., and Jones, J.G. (2022). De novo lipogenesis in non-alcoholic fatty liver disease: Quantification with stable isotope tracers. Eur. J. Clin. Invest. *52*, e13733. https://doi.org/10.1111/eci.13733.
75. Knebel, B., Fahlbusch, P., Dille, M., Wahlers, N., Hartwig, S., Jacob, S., Kettel, U., Schiller, M., Herebian, D., Koellmer, C., et al. (2019). Fatty Liver Due to Increased de novo Lipogenesis: Alterations in the Hepatic Peroxisomal Proteome. Front. Cell Dev. Biol. *7*, 248. https://doi.org/10.3389/fcell.2019.00248.
76. Schwarz, J.-M., Clearfield, M., and Mulligan, K. (2017). Conversion of Sugar to Fat: Is Hepatic de Novo Lipogenesis Leading to Metabolic Syndrome and Associated Chronic Diseases? J. Am. Osteopath. Assoc. *117*, 520–527. https://doi.org/10.7556/jaoa.2017.102.
77. Zhao, J., Qi, Y.F., and Yu, Y.R. (2021). STAT3: A key regulator in liver fibrosis. Ann. Hepatol. *21*, 100224. https://doi.org/10.1016/j.aohep.2020.06.010.
78. Benhammou, J.N., Ko, A., Alvarez, M., Kaikkonen, M.U., Rankin, C., Garske, K.M., Padua, D., Bhagat, Y., Kaminska, D., Kärjä, V., et al. (2019). Novel Lipid Long Intervening Noncoding RNA, Oligodendrocyte Maturation-Associated Long Intergenic Noncoding RNA, Regulates the Liver Steatosis Gene Stearoyl-Coenzyme A Desaturase As an Enhancer RNA. Hepatol. Commun. *3*, 1356–1372. https://doi.org/10.1002/hep4.1413.
79. Männistö, V., Kaminska, D., Käkelä, P., Neuvonen, M., Niemi, M., Alvarez, M., Pajukanta, P., Romeo, S., Nieuwdorp, M., Groen, A.K., and Pihlajamäki, J. (2021). Protein Phosphatase 1 Regulatory Subunit 3B Genotype at rs4240624 Has a Major Effect on Gallbladder Bile Composition. Hepatol. Commun. *5*, 244–257. https://doi.org/10.1002/hep4.1630.
80. McCarthy, D.J., Chen, Y., and Smyth, G.K. (2012). Differential expression analysis of multifactor RNA-Seq experiments with respect to biological variation. Nucleic Acids Res. *40*, 4288–4297. https://doi.org/10.1093/nar/gks042.
81. Chella Krishnan, K., Sabir, S., Shum, M., Meng, Y., Acín-Pérez, R., Lang, J.M., Floyd, R.R., Vergnes, L., Seldin, M.M., Fuqua, B.K., et al. (2019). Sex-specific metabolic functions of adipose Lipocalin-2. Mol. Metabol. *30*, 30–47. https://doi.org/10.1016/j.molmet.2019.09.009.
82. Chella Krishnan, K., Vergnes, L., Acín-Pérez, R., Stiles, L., Shum, M., Ma, L., Mouisel, E., Pan, C., Moore, T.M., Péterfy, M., et al. (2021). Sex-specific genetic regulation of adipose mitochondria and metabolic syndrome by Ndufv2. Nat. Metab. *3*, 1552–1568. https://doi.org/10.1038/s42255-021-00481-w.
83. Bennett, B.J., Farber, C.R., Orozco, L., Kang, H.M., Ghazalpour, A., Siemers, N., Neubauer, M., Neuhaus, I., Yordanova, R., Guan, B., et al. (2010). A high-resolution association mapping panel for the dissection of complex traits in mice. Genome Res. *20*, 281–290. https://doi.org/10.1101/gr.099234.109.
84. Parks, B.W., Sallam, T., Mehrabian, M., Psychogios, N., Hui, S.T., Norheim, F., Castellani, L.W., Rau, C.D., Pan, C., Phun, J., et al. (2015). Genetic architecture of insulin resistance in the mouse. Cell Metabol. *21*, 334–347. https://doi.org/10.1016/j.cmet.2015.01.002.
85. Folch, J., Lees, M., and Sloane Stanley, G.H. (1957). A simple method for the isolation and purification of total lipides from animal tissues. J. Biol. Chem. *226*, 497–509.
86. Dobin, A., Davis, C.A., Schlesinger, F., Drenkow, J., Zaleski, C., Jha, S., Batut, P., Chaisson, M., and Gingeras, T.R. (2013). STAR: ultrafast universal RNA-seq aligner. Bioinformatics *29*, 15–21. https://doi.org/10.1093/bioinformatics/bts635.
87. Love, M.I., Anders, S., Kim, V., and Huber, W. (2015). RNA-Seq workflow: gene-level exploratory analysis and differential expression. F1000Res. *4*, 1070. https://doi.org/10.12688/f1000research.7035.1.
88. Wu, T., Hu, E., Xu, S., Chen, M., Guo, P., Dai, Z., Feng, T., Zhou, L., Tang, W., Zhan, L., et al. (2021). clusterProfiler 4.0: A universal enrichment tool for interpreting omics data. Innovation *2*, 100141. https://doi.org/10.1016/j.xinn.2021.100141.
89. Livak, K.J., and Schmittgen, T.D. (2001). Analysis of relative gene expression data using real-time quantitative PCR and the 2(-Delta Delta C(T)) Method. Methods *25*, 402–408. https://doi.org/10.1006/meth.2001.1262.
90. Vandesompele, J., De Preter, K., Pattyn, F., Poppe, B., Van Roy, N., De Paepe, A., and Speleman, F. (2002). Accurate normalization of real-time quantitative RT-PCR data by geometric averaging of multiple internal control genes. Genome Biol. *3*, RESEARCH0034. https://doi.org/10.1186/gb-2002-3-7-research0034.

STAR★METHODS

KEY RESOURCES TABLE

REAGENT or RESOURCE	SOURCE	IDENTIFIER
Antibodies		
rabbit monoclonal ITIH3	SinoBiological	Cat# 16138-R049
rabbit monoclonal STAT1	Cell Signaling	Cat# 14994; RRID: AB_2737027
rabbit monoclonal Phospho-STAT1 (Ser727)	Cell Signaling	Cat# 8826; RRID: AB_2773718
rabbit polyclonal STAT3	Proteintech	Cat# 10253-2-AP; RRID: AB_2302876
rabbit monoclonal Phospho-STAT3 (Tyr705)	Cell Signaling	Cat# 9145; RRID: AB_2491009
rabbit monoclonal JAK1	Cell Signaling	Cat# 3344; RRID: AB_2265054
mouse monoclonal ACTIN	abcam	Cat# ab8226; RRID: AB_306371
rabbit monoclonal GAPDH	Cell Signaling	Cat# 5174; RRID: AB_10622025
Bacterial and virus strains		
AAV8.TBG.PI.mItih3.rBG	Penn Vector Core facility	N/A
AAV8.TBG.PI.eGFP.rBG	Penn Vector Core facility	N/A
AAV8.TBG.PI.shItih3.rBG	Penn Vector Core facility	N/A
AAV8.TBG.PI.shFFluc.rBG	Penn Vector Core facility	N/A
Chemicals, peptides, and recombinant proteins		
Human ITIH3	SinoBiological	Cat# 16138-H08H
QIAzol Lysis Reagent	Qiagen	Cat# 79306
Chloroform, HPLC grade	Thermo Fisher	Cat# C606-4
Isopropanol, 99.5%, for molecular biology	Acros Organics	Cat# 32727-0010
Oleic Acid-Albumin from bovine serum	Sigma-Aldrich	Cat# O3008-5ML
High fat/high sucrose (HF/HS) diet	Research Diets	Cat# D12266B
Critical commercial assays		
miRNeasy Mini Kit	Qiagen	Cat# 217004
High-Capacity cDNA Reverse Transcription Kit	Thermo Fisher	Cat# 4368813
PowerUp SYBR Green Master Mix	Thermo Fisher	Cat# A25778
Serum Triglyceride Determination Kit	Sigma-Aldrich	Cat# TR0100-1KT
Cholesterol Quantitation Kit	Sigma-Aldrich	Cat# MAK043-1KT
Phospholipids C	Wako Diagnostics	Cat# 997-01801
Glucose Liquid Reagent for Diagnostic Set	Thermo Fisher	Cat# SB-1070-125
Mouse Ultrasensitive Insulin ELISA Jumbo	ALPCO	Cat# 80-INSMSU-E10
Deposited data		
Chow HMDP liver	GEO	GSE16780
HF/HS HMDP liver	GEO	GSE64769
Western HMDP liver	GEO	GSE66568
Experimental models: Cell lines		
AML12	ATCC	Cat# CRL-2254; RRID: CVCL_0140
Experimental models: Organisms/strains		
C57BL6J, male, 8 weeks old	Jackson Laboratories	RRID: IMSR_JAX:000664
Oligonucleotides		
B2m-Forward: TACGTAACACAGTTCCACCCGCCTC	This paper	N/A

(*Continued on next page*)

Continued

REAGENT or RESOURCE	SOURCE	IDENTIFIER
B2m-Reverse: GCAGGTTCAAATGAATCTTCAGAGCATC	This paper	N/A
Tbp-Forward: CAAACCCAGAATTGTTCTCCTT	This paper	N/A
Tbp-Reverse: ATGTGGTCTTCCTGAATCCCT	This paper	N/A
Itih3-Forward: TGCTCACAATGTTGTCACCAC	This paper	N/A
Itih3-Reverse: CTTGACCAAACCGGCTGTC	This paper	N/A
Fasn-Forward: TGCACCTCACAGGCATCAAT	This paper	N/A
Fasn-Reverse: GTCCCACTTGATGTGAGGGG	This paper	N/A
Elovl6-Forward: GAAAAGCAGTTCAACGAGAACG	This paper	N/A
Elovl6-Reverse: AGATGCCGACCACCAAAGATA	This paper	N/A
Scd1-Forward: TTCCCTCCTGCAAGCTCTAC	This paper	N/A
Scd1-Reverse: CAGAGCGCTGGTCATGTAGT	This paper	N/A
Software and algorithms		
R software environment for analyses	https://www.r-project.org/	N/A
DESeq2	https://bioconductor.org/packages/release/bioc/html/DESeq2.html	N/A
clusterProfiler	https://bioconductor.org/packages/release/bioc/html/clusterProfiler.html	N/A
DAVID	https://david.ncifcrf.gov/	N/A
ToppGene	https://toppgene.cchmc.org/	N/A

RESOURCE AVAILABILITY

Lead contact

Further information and requests for resources and reagents should be directed to and will be fulfilled by the Lead Contact, Karthickeyan Chella Krishnan (chellakn@ucmail.uc.edu).

Materials availability

This study did not generate new unique reagents.

Data and code availability

- All HMDP liver microarray raw data can be accessed at the Gene Expression Omnibus under the accession numbers: GSE16780, GSE64769 and GSE66568.
- This paper does not report original code.
- Any additional information required to reanalyze the data reported in this paper is available from the lead contact upon request.

EXPERIMENTAL MODEL AND STUDY PARTICIPANT DETAILS

Animals

All mice were purchased from the Jackson Laboratory and bred at UCLA and University of Cincinnati according to approved IACUC protocols. Animal health was monitored daily by vivarium personnel and were maintained under standard housing condition with 12 h light/dark cycle. For steatosis models, 8-week-old male mice were fed a high fat/high sucrose (HF/HS) diet (Research Diets-D12266B) for 8 weeks or 15% w/v fructose in drinking water for 12 weeks.

Human population cohort

The study detail and its characteristics have been reported elsewhere[78,79] and in Table S3. The study included a total of 262 participants of the Kuopio Obesity Surgery (KOBS) study who underwent the Roux-en-Y gastric bypass surgery at Kuopio University Hospital, and from whom

both detailed liver histology and RNA sequencing data were available. Total RNA was extracted and purified using the miRNeasy Mini Kit (Qiagen). RNA sequencing libraries underwent 50-nucleotide long paired-end sequencing on Illumina HiSeq 2500 machine, followed by read alignment, normalization and differential expression analysis considering the technical and confounding factors (namely RIN, uniquely aligned reads %, 3' bias, age, sex, and BMI) as described previously.[79] The gene level count values were normalized using a trimmed-mean of M values converted to count per million using edgeR[80] and inverse normal transformed. The study protocol was approved by the Ethics Committee of the Northern Savo Hospital District. It was performed in accordance with the Helsinki Declaration. Written informed consent was obtained from all the participants.

AAV expression system

Liver ITIH3 gene expression was modulated by AAV-mediated gene transfer, as described, and successfully applied in our previous studies.[44,81,82] For ITIH3 overexpression, the cDNA of ITIH3 (NM_008407.2) was cloned into the AAV8 expression plasmid under a TBG promoter. For ITIH3 deficiency, the AAV8-TBG vector expressing shRNA sequences against ITIH3 (TTGGCAACAATCTGAATTATAA) was created as previously described.[44,81] All AAV syntheses were performed on a fee-for-service basis at the University of Pennsylvania's Penn Vector Core facility.

ITIH3 loss- and gain-of-function studies

Eight-week-old male C57BL/6J mice were intraperitoneally injected with respective AAVs (~1×10^{12} genome copies diluted in 200 μL saline). We injected control mice with AAVs expressing shRNA against firefly luciferase gene (for knockdown) or GFP (for overexpression). After this, the mice were subjected to 8 weeks of HF/HS diet or 12 weeks of 15% w/v fructose in drinking water. Body weight and body composition were measured for every two weeks until euthanasia. On the last day of the experiment, mice were fasted for 4 h and animals were euthanized, and tissues were collected. For analyzing plasma lipids, retro-orbital blood was collected, and plasma was separated. Liver tissues were collected for weight, mitochondria isolation, lipid measurements, histology and RNA and protein isolation.

METHOD DETAILS

HMDP liver gene expression analysis

Snap frozen liver tissues of HMDP mice maintained on regular chow (healthy)[83] or HF/HS (steatosis)[39] or western diet (NASH/fibrosis)[40] were used for RNA isolation. Global gene expression analysis was done by using Affymetrix HT_MG430A arrays, and filtering criteria for microarray data was done as previously described.[84]

Liver and plasma lipid analysis

Liver lipids were extracted as described,[85] while plasma was directly used. Calorimetric assays from Sigma (triglyceride, total cholesterol and unesterified cholesterol) and Wako (phospholipids) were used to measure respective lipids according to the manufacturer's instructions.

Isolation of liver mitochondria and bioenergetics

Mitochondria were isolated from liver tissue and respiration was measured as described.[15,44] Briefly, mitochondria were obtained by dual centrifugation and resuspended in respiration buffer, while mitochondrial protein was estimated by BCA method. Seahorse XF Pro Analyzer (Agilent) was used to measure mitochondrial respiration. For Complex I respiration, 5 mM pyruvate (Complex I substrate), 0.5 mM malate and 4 mM ADP were used. For Complex II respiration, 5 mM succinate (Complex II substrate), 2μM rotenone (Complex I inhibitor) and 4 mM ADP were used. Then, oxygen consumption rates (OCR) were measured before and after the sequential injections of 2.5μM oligomycin, 4μM FCCP, and 1μM of rotenone/antimycin A. Measures were normalized by total protein.

Cellular bioenergetics

Cellular bioenergetics on AML12 (male) cells were performed as described.[15,82] Briefly, GFP or ITIH3 transfected cells and control or exogenous rhITIH3 treated cells were plated on XF cell culture plate (10,000 cells per well) and OCR were measured before and after the sequential injections of 1.5μM oligomycin, 1μM FCCP, and 0.5μM of rotenone/antimycin A. Measures were normalized by cell number.

RNA isolation, Library Preparation, and sequencing

Flash-frozen liver samples were homogenized in QIAzol (Qiagen), and after chloroform phase separation, RNA was isolated according to the manufacturer's protocol using miRNeasy columns (Qiagen). Libraries were prepared from these extracted liver RNA (Agilent Bioanalyzer RIN >7) using NEBNext Ultra II Directional RNA Library Prep kit (New England Biolabs) per the manufacturers' instructions. The pooled libraries were sequenced with an Illumina NextSeq 2000 instrument (Illumina) by the Genomics, Epigenomics, and Sequencing Core (GESC) at the University of Cincinnati. Reads were aligned to the mouse genome mm10 using STAR aligner[86] and quantified using the Bioconductor R packages as described in the RNA-seq workflow.[87] Follow up enrichment analyses were done using DAVID[41] and ToppGene.[42] Gene set enrichment analysis (GSEA) was performed using the clusterProfiler R package.[88]

RNA isolation for qPCR

First, total RNA from frozen liver tissues or AML12 cells was extracted using TRIzol (Invitrogen). Next, first-strand complementary DNA (cDNA) was made using High-Capacity cDNA Reverse Transcription Kit (Applied Biosystems) following manufacturer's instructions. Finally, PowerUp SYBR Green Master Mix (Applied Biosystems) was used to measure relative normalized expression using the $2^{-\Delta\Delta Ct}$ method.[89] The geometric mean of *B2m* and *Tbp* was used for normalization as described.[90] All qPCR primer sequences are listed in key resources table.

Immunoblotting analyses

Liver lysates were prepared in RIPA buffer (Teknova) and proteins were resolved in 4%–12% Bis-Tris gels (Invitrogen). Proteins were then transferred to polyvinylidene difluoride (PVDF) membrane (Thermo Scientific) and probed by using rabbit monoclonal ITIH3 (SinoBiological #16138-R049), rabbit monoclonal STAT1 (Cell Signaling #14994), rabbit monoclonal Phospho-STAT1 (Ser727) (Cell Signaling #8826), rabbit polyclonal STAT3 (Proteintech #10253-2-AP), rabbit monoclonal Phospho-STAT3 (Tyr705) (Cell Signaling #9145), rabbit monoclonal JAK1 (Cell Signaling #3344), mouse monoclonal ACTIN (abcam #ab8226) and rabbit monoclonal GAPDH (Cell Signaling #5174), and their respective secondary antibodies. Bands were quantified by using ImageJ.

QUANTIFICATION AND STATISTICAL ANALYSIS

Statistical analysis

Graphs and statistical analyses were performed using Prism v10.0.2 (GraphPad Software). Errors bars plotted on graphs are presented as the mean $\pm$ standard error of the mean (SEM) unless reported otherwise. The critical significance value (α) was set at 0.05, and if the p values were less than α, we reported that by rejecting the null hypothesis, the observed differences were statistically significant.